Insights into polyprotein processing and RNA-protein interactions in foot-and-mouth disease virus genome replication.

Danielle M. Pierce, David J. Rowlands, Nicola J. Stonehouse* and Morgan R. Herod*

School of Molecular and Cellular Biology, Faculty of Biological Sciences and Astbury Centre for Structural Molecular Biology, University of Leeds, Leeds, United Kingdom

* Corresponding author's: m.r.herod@leeds.ac.uk; n.j.stonehouse@leeds.ac.uk

Running title: Polyprotein processing regulates FMDV replication

Keywords: FMDV, picornavirus, cleavage, replication, replication complex

Word count: Abstract 229 words; Importance 150 words; Main text 5465; 7 figures

Abstract

Foot-and-mouth disease affects cloven hoofed animals and is caused by foot-and-mouth disease virus (FMDV), a picornavirus with a positive-sense RNA genome. The FMDV genome contains a single open reading frame, which is translated to produce a polyprotein that is cleaved by viral proteases to produce the viral structural and non-structural proteins. Initial processing of the polyprotein occurs at three main junctions to generate four primary products; L^{pro} and the P1, P2 and P3 precursors (also termed 1ABCD, 2BC and $3AB_{1,2,3}CD$). The 2BC and $3AB_{1,2,3}CD$ precursors undergo subsequent proteolysis to generate non-structural proteins that are required for viral replication, including the enzymes 2C, $3C^{pro}$ and $3D^{pol}$. These precursors can be processed through both *cis* and *trans* (i.e., intra- and inter-molecular proteolysis) pathways, which are thought to be important for controlling virus replication. Our previous studies suggested that a single residue in the $3B_3$-3C junction had an important role in controlling $3AB_{1,2,3}CD$ processing. Here, we use *in vitro* based

assays to show that a single point mutation at the $3B_3$-3C boundary increases the rate of proteolysis to generate a novel 2C-containing precursor. Complementation assays showed that while this point mutation permitted production of some non-enzymatic non-structural proteins, those with enzymatic functions were inhibited. Interestingly, replication could only be supported by complementation with mutations in *cis* acting RNA elements, providing genetic evidence for a functional interaction between replication enzymes and RNA elements.

Importance

Foot-and-mouth disease virus (FMDV) is an economically important pathogen of animals that is responsible for foot-and-mouth disease (FMD). FMD is endemic in many parts of the world and can results in major economic losses. Replication of the virus is a highly coordinated event that occurs within membrane-associated compartments in infected cells and requires the viral non-structural proteins. These are all initially produced as a polyprotein that undergoes proteolysis likely through both *cis* and *trans* pathways (i.e., intra- and inter-molecular proteolysis). Alternative processing pathways can provide a mechanism to help coordinate viral replication by providing temporal control to protein production. Here, we analyse the consequences of mutations that change temporal control of FMDV polyprotein processing. Our data suggests that correct processing is required to produce key enzymes for replication in an environment in which they can interact with essential viral RNA elements. These data further the understanding of FMDV genome replication.

Introduction

Small RNA viruses have limited genome sequence space and therefore minimal coding capacity. These viruses have evolved several strategies to overcome this limitation, including the use of protein precursors that can perform different functions to the mature proteins. Individual proteins and their precursors can also sometimes perform more than one function (1). Examples are the 3CD and 2BC precursors from poliovirus (PV) and foot-and-mouth disease virus (FMDV), respectively, both members of the *Picornaviridae* family. The 3CD protein is involved in priming genome replication, whilst also having protease activity and the $3C^{pro}$ and $3D^{pol}$ cleavage products have protease and RNA-dependent RNA polymerase activities, respectively (1). Likewise, the FMDV 2BC precursor inhibits the secretory pathway, a function apparently independent of the roles of 2B as a viroporin and 2C as a viral ATPase (2-4).

The *Picornaviridae* family includes several important human and animal pathogens, including but not limited to PV and FMDV. PV is responsible for the incapacitating (and potentially fatal) human disease poliomyelitis, while FMDV is the causative agent of foot-and-mouth disease, an acute vesicular disease of cloven-hoofed ruminants including livestock, which can be economically-damaging. The FMDV genome contains a single open reading frame that produces a ~250 kDa polyprotein (5). Initial processing of the FMDV polyprotein occurs at three positions to produce four primary products: L^{pro}, the capsid precursor P1-2A and two non-structural protein precursors 2BC (also termed P2) and $3AB_{1,2,3}CD$ (also termed P3) (6, 7). L^{pro} is autocatalytically released from the N-terminal region of the polyprotein (6, 8). The P1-2A precursor is released from the polyprotein via a co-translational 2A-driven ribosome skipping mechanism (9) before the 2BC-$3AB_{1,2,3}CD$ polyprotein is

processed by $3C^{pro}$. For FMDV, initial processing is believed to be predominantly at the 2C-3A junction, generating 2BC and $3AB_{1,2,3}CD$ precursors. Further $3C^{pro}$-mediated proteolysis releases the final proteins via a succession of intermediate precursors (7, 10, 11). Processing of the 2BC precursor ultimately generates the 2B and 2C proteins, both of which have multiple roles in replication.The $3AB_{1,2,3}CD$ precursor is composed of the transmembrane protein 3A, three 3B peptides (individually referred to as $3B_1$, $3B_2$ and $3B_3$), the protease $3C^{pro}$, and the polymerase $3D^{pol}$ (12, 13).

Processing of the non-structural polyprotein by $3C^{pro}$ is thought to occur through at least two separate pathways to generate mutually-exclusive sets of precursors (14). For example, for FMDV, the $3AB_{1,2,3}CD$ precursor is processed to generate the precursors $3AB_{1,2,3}C$ and 3CD, which must be derived from alternative processing strategies. Likewise, for PV, the 3ABCD precursor (the equivalent of $3AB_{1,2,3}CD$ in FMDV) can be processed to generate 3ABC and 3CD. Furthermore, it appears that this alternative processing may be temporally controlled and used to regulate virus replication. For example, previous studies with PV have demonstrated that later production of 3AB and 3CD can delay the initiation of viral RNA replication (15). For FMDV, reducing cleavage of 3CD inhibits replication by limiting the supply of $3D^{pol}$ (16, 17). Processing through alternative pathways is likely to be driven (in part) through a switch between intra-molecular vs inter-molecular proteolysis (i.e., *cis* vs *trans* cleavage events). However, methods to differentiate between these *cis* vs *trans* cleavages events are challenging and as a result the mechanism(s) that controls this switch are not completely understood.

Like all positive-sense RNA viruses, picornavirus genome replication is associated with virus-induced cytoplasmic membranous structures, sometimes referred to as

"replication complexes" or "replication organelles" (18). In these assemblies, multiple new viral positive-strand RNAs are synthesised via a complementary negative-sense template. For FMDV the full composition of these assemblies is unknown, but they are likely composed of multiple viral and cellular factors, including the non-structural proteins 3B, $3D^{pol}$ and 3CD. Some of the viral non-structural proteins and precursors associate with RNA elements located in the 5' and 3' untranslated regions (UTRs) that flank the open reading frame (5). The 5' UTR of FMDV is uncharacteristically long for a picornavirus and contains several distinct structural elements, including an internal ribosome entry site (IRES), a *cis*-acting replicative element (*cre*) and a large stem loop (termed the S-fragment) (19-22). The IRES has been well studied and is used to initiate protein translation in a cap-independent manner (20, 21). The *cre* is essential for replication and acts as the template for uridylation of 3B (also known as VPg) to generate the replicative primer, VPg-pUpU (23-28). The role of the S-fragment in FMDV replication is less well understood but may be involved in both replication and modulating the innate immune response (29). In other picornaviruses, such as PV, an RNA structure termed the cloverleaf (or oriL) is located at the 5' terminus of the genome at the site occupied by the S-fragment stem-loop in FMDV (30). This interacts with the precursor protein 3CD as well as host proteins and is involved in initiating negative-strand RNA synthesis (31-36). Furthermore, for PV, other precursor proteins have also been implicated in 5' UTR interactions, including 3AB (the equivalent to $3AB_{1,2,3}$ in FMDV), 3BCD and 3ABCD, and have been suggested to be important for controlling replication (15, 32, 37, 38). The role of precursors in FMDV replication is less well established.

In a previous study, we used an FMDV replicon system, where replication is monitored by fluorescent protein (e.g., GFP/RFP) expression over time, to

investigate FMDV replication by mutation of the 3B proteins (16). We reported a series of amino acid substitutions that increased the efficiency of processing at the $3B_3$-3C junction but inhibited replication by abrogating the release of free $3D^{pol}$. Simultaneously, we observed that these mutations caused an overall shift in $3AB_{1,2,3}CD$ processing and channelled precursor synthesis mainly down one pathway generating $3AB_{1,2,3}$ and 3CD precursors. This series of mutations has enabled us to separate alternative cleavage pathways and study the function of different precursor sets. Here, we investigated the mechanism by which these mutations result in increased processing between $3B_3$ and 3C. Our data suggest that a single amino acid substitution increases sensitivity to *trans*-mediated proteolysis at this boundary. Furthermore, when placed into the context of a full-length polyprotein, this single substitution resulted in accumulation of a novel precursor. Interestingly, it also prevented reciprocal complementation of replicons *in trans*, which we demonstrate is due to a deficiency in the functions of essential viral enzymes.

Results

A single point mutation in $3B_3$ prevents replicon replication.

In a previous study, we reported that mutations within $3B_3$, at the boundary with $3C^{pro}$, dramatically changed processing of the FMDV $3AB_{1,2,3}CD$ polyprotein and prevented release of active $3D^{pol}$. However, through blind passage a compensatory mutation was selected which restored replication and wild-type (WT) $3AB_{1,2,3}CD$ processing. This was identified as a reversion of a lysine at the P2 residue of the $3B_3$-3C junction to the WT threonine (15). These data suggested that the amino acid in the P2 position of the $3B_3$-3C junction alone can be a major determinant of altered polyprotein processing.

Before investigating the mechanism by which mutations at this junction increased processing, we first sought to establish that this residue alone was sufficient to change FMDV polyprotein processing and prevent replicon replication. To this end, we generated an FMDV replicon with a threonine to lysine mutation at the P2 residue of the $3B_3$-3C cleavage junction (Figure 1A and B). In this replicon (termed, ptGFP-$3B_3^{T>K}$) the reporter protein ptGFP replaced the structural proteins, allowing ptGFP expression to be used as an indicator of replicon replication (Figure 1A). This replicon RNA was transfected into BHK-21 cells alongside the previously published mutant replicons ptGFP-$3B_{1,2,3}^{Y3F}$ (contains inactivating point mutations to the triptych of 3B genes) and ptGFP-$3B_{3/2}$ (the six C-terminal residues of $3B_3$ replaced by those of $3B_2$) (Figure 1B). A WT ptGFP expressing replicon (ptGFP) and a replicon containing an inactivating double point mutation in $3D^{pol}$ (ptGFP-$3D^{GNN}$) were included as controls. The latter replicon serves as a negative control for ptGFP production from translation of the input transfected RNA, as we have previous described (39). RNAs from these replicons were transfected into BHK-21 cells and

replication monitored by ptGFP fluorescence using an Incucyte real-time imaging system (Figure 1C).

As anticipated, the WT ptGFP replicon produced ptGFP >100-fold greater than the ptGFP-3D^{GNN} control replicon, as previously reported. In comparison the ptGFP-3B$_3^{T>K}$ replicon showed GFP expression equivalent to the replication-defective ptGFP-3D^{GNN} control. These data were in agreement with those obtained with the ptGFP-3B$_{3/2}$ and ptGFP-3B$_{1,2,3}^{Y3F}$ replication-defective replicons we previously reported (16). Thus, the 3B$_3^{T>K}$ mutation alone is sufficient to prevent replicon replication.

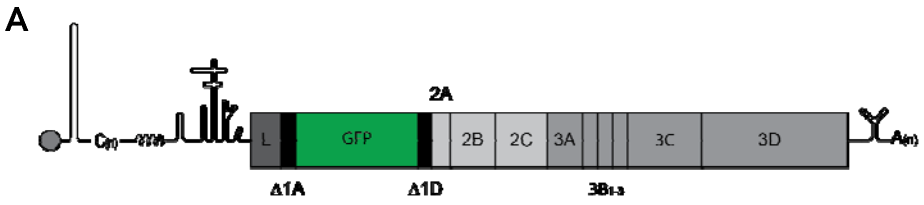

B

$3B_2$	GPYAGPMERQKPLKVKAKAPVVKE
$3B_3$	GPYEGPVKKPVALKVKAKNLIVTE
$3B_{3/2}$	GPYEGPVKKPVALKVKAK**APVVKE**
$3B_3^{T>K}$	GPYEGPVKKPVALKVKAKNLIV**K**E

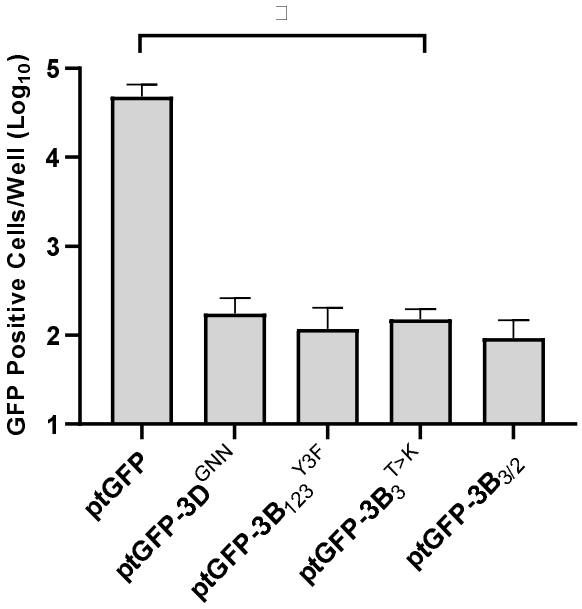

Figure 1. A single mutation at the $3B_3$-3C junction prevents FMDV replicon replication. (A) Schematic diagram of the FMDV replicon. **(B)** Sequence alignments of the 3B cleavage junctions with the $3B_{3/2}$ and $3B_3^{T>K}$ mutants. **(C)** Replication of replicons containing $3B_3$ mutations as well as the WT ptGFP replicon (ptGFP) and replication-defective controls containing inactivating mutations in $3D^{pol}$ ($3D^{GNN}$), or 3B proteins ($3B_{1,2,3}^{Y3F}$). GFP expression was monitored hourly for 24 hours. The graph shows GFP positive cells per well at 8 hours post-transfection when replication is maximal. Significance compared to WT control (n = 3 ± SEM; * = $p \leq 0.05$).

A single mutation at the $3B_3$-3C boundary increases the rate of proteolysis.

We previously demonstrated that the ptGFP-$3B_{3/2}$ mutation inhibited replication and changed processing of the $3AB_{1,2,3}CD$ polyprotein. To confirm that the $3B_3^{T>K}$ substitution was sufficient to induce the same changes, we employed the previously described *in vitro* coupled transcription/translation assay (16). T7 expression constructs were generated to express either the WT FMDV polyprotein or a polyprotein containing the $3B_3^{T>K}$ point mutation. The polyprotein used in these experiments included 2BC as well as the $3AB_{1,2,3}CD$ region to determine changes to the entire NS polyprotein. These experiments also included a control polyprotein containing an inactivating mutation in $3C^{pro}$ ($3C^{C163A}$) predicted to prevent its proteolytic activity (40). Processing was investigated by [^{35}S] methionine/cysteine pulse/chase labelling in *in vitro* coupled transcription/translation reactions, harvesting samples at regular time points and analysing protein products by SDS-PAGE (Figure 2A and B).

For the WT construct, the full-length $3AB_{1,2,3}CD$ precursor was detected at early time points, and was steadily processed over time primarily into $3AB_{1,2,3}C$ and $3D^{pol}$, with a small amount of 3CD derived from an alternative processing pathway. At the later time points (40 and 60 minutes), $3AB_{1,2,3}$ was also detected. Both 2B and 2C were present, in addition to a limited amount of the precursor 2BC at earlier time points. When compared to WT, the construct containing the $3B_3^{T>K}$ mutation resulted in greater amounts of the 3CD and $3AB_{1,2,3}$ precursors and less of the $3AB_{1,2,3}CD$ precursor and $3D^{pol}$. There were also increased levels of the 2BC precursor in addition to a high molecular weight precursor, possibly $2BC3AB_{1,2,3}$, which was detected at early time points and gradually decreased over time. These data extended our previous observations demonstrating that the $3B_3^{T>K}$ substitution alone

is sufficient to accelerate proteolysis at the $3B_3$-3C junction and so increases the relative amounts of 2BC, 3CD and $3AB_{1,2,3}$.

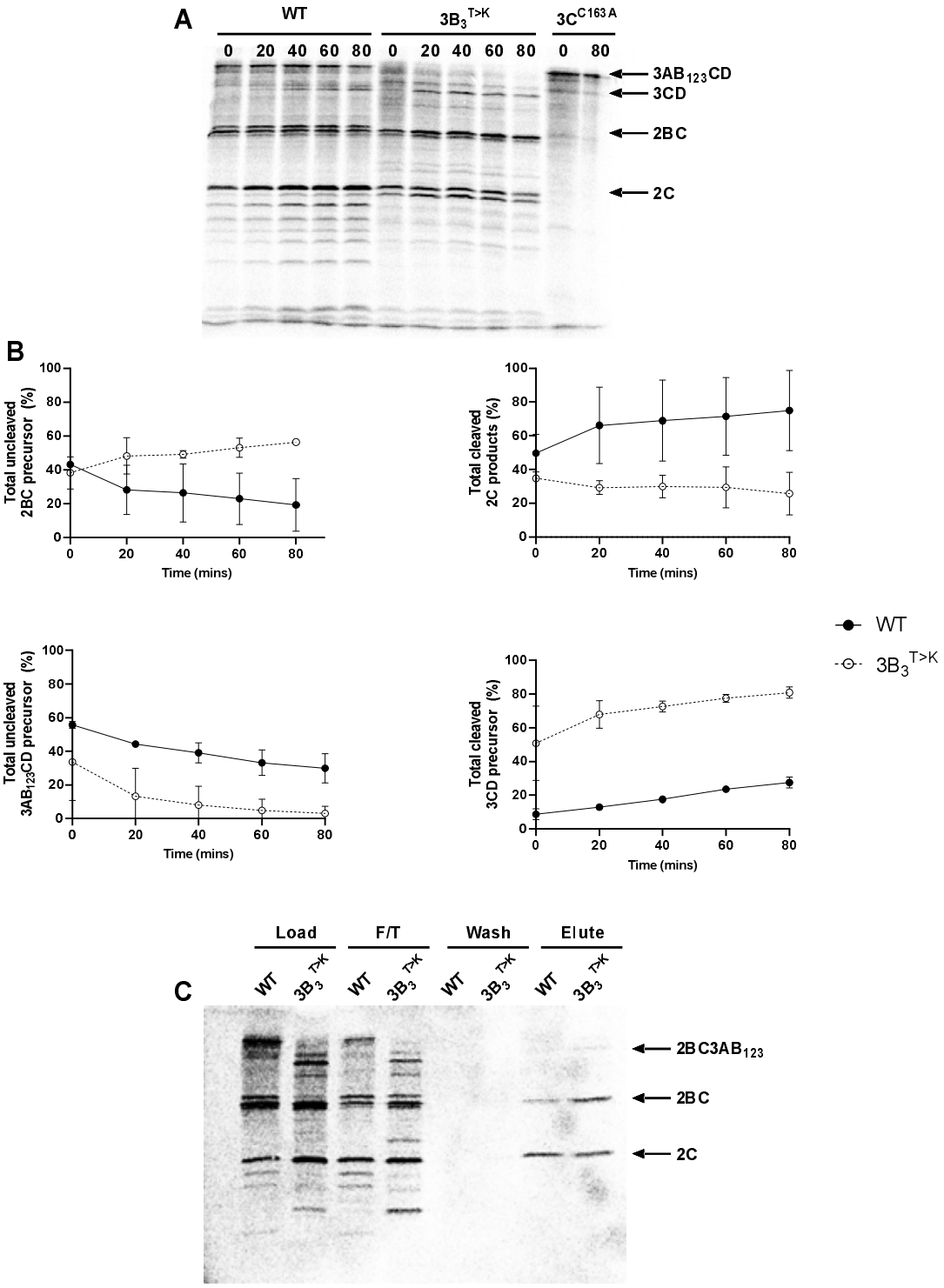

Figure 2. A single mutation at the $3B_3$-3C boundary increases the rate of proteolysis and drives the production of novel precursors. (A) Plasmids expressing the WT or mutant $3B_3^{T>K}$ FMDV polyprotein precursors were used to

prime [^{35}S] labelled pulse-chase *in vitro* coupled transcription/translation reactions. At regular intervals samples were taken and stopped by the addition of 2 x Laemmli buffer. Proteins were separated by SDS-PAGE and visualised by autoradiography. The identity of some FMDV proteins is shown. **(B)** The percentage of protein or protein precursor was quantified as a total percentage of 2C or 3D^{pol} containing products, as appropriate (n = 2 ± SD). **(C)** Duplicate reactions were incubated for 90 minutes before immunoprecipitation of 2C containing precursors with anti-2C antibodies. The pre- and post-precipitation samples were separated by SDS-PAGE and visualised by autoradiography. Arrows show the identity of 2C containing proteins, based on predicted molecular weights.

Increasing polyprotein proteolysis generates a novel 2BC containing precursor.

The previous *in vitro* translation experiments suggested that the $3B_3^{T>K}$ mutation increased the production of the 2BC precursor in addition to a larger molecular weight precursor not observed in the WT control. To confirm the identity of the 2C-containing precursors the *in vitro* translation samples were immunoprecipitated using an anti-2C antibody. T7 constructs expressing the WT polyprotein or polyprotein containing the $3B_3^{T>K}$ substitution were used in *in vitro* coupled transcription/translation reactions with [^{35}S] methionine/cysteine pulse/chase labelling. Samples were taken after 90 minutes and immunoprecipitation performed on half of the sample. Both pre- and post-immunoprecipitation protein samples were analysed by SDS-PAGE (Figure 2C).

In comparison to WT, a smaller proportion of mature 2C (but more unprocessed 2BC precursor) were immunoprecipitated with an anti-2C antibody following expression from the polyprotein containing the $3B_3^{T>K}$ mutation. Furthermore, the additional higher molecular weight band which was only present following expression of the $3B_3^{T>K}$ precursor was also immunoprecipitated with the anti-2C antibody. Based on these observations and the estimated molecular weight, this product is mostly likely a $2BC3AB_{1,2,3}$ precursor. These results agree with previous data and suggest that the $3B_3^{T>K}$ mutation preferentially increases the rate of proteolysis at the $3B_3$-3C junction, compared to the 2C-3A junction, resulting in the accumulation of $2BC3AB_{1,2,3}$, which is not normally detected.

The $3B_3^{T>K}$ substitution stimulates *trans*-mediated processing.

We speculated that there were two likely mechanisms by which the order of polyprotein processing was altered. It is possible that the point mutation affected

protein folding conformations to change the order of *cis*-mediated proteolysis such that the mutant $3B_3^{T>K}$ boundary was processed first. However, we believe the more likely possibility is that the point mutation generated a boundary sequence that was preferentially recognised *in trans* by $3C^{pro}$ and/or a $3C^{pro}$-containing precursor. To explore the latter possibility, we adapted our *in vitro* assay to investigate *trans*-mediated cleavage. For simplicity, we adapted both the WT $3AB_{1,2,3}CD$ precursor or precursor containing the $3B_3^{T>K}$ substitution to also contain the inactivating mutation in $3C^{pro}$ ($3C^{C163A}$) to prevent self-proteolysis (40). These precursor substrates (termed $3C^{C163A}$ and $3B_3^{T>K}$-$3C^{C163A}$, respectively) were translated *in vitro* with [^{35}S] methionine/cysteine before adding excess unlabelled methionine/cysteine and purified active $3C^{pro}$ to a duplicate set of reactions (plus $3C^{pro}$). Samples were harvested at regular time points and processing of the [^{35}S] labelled precursor was analysed by SDS-PAGE (Figure S1). As controls, the experiment was conducted with the WT and $3B_3^{T>K}$ constructs that did not contain the $3C^{C163A}$ point mutation (Figure S1). To aid interpretation the relative amount of $3AB_{1,2,3}CD$ and 3CD products was quantified by phosphorimaging (Figure 3).

Both WT and $3B_3^{T>K}$ precursors carrying the $3C^{C163A}$ mutation produced only uncleaved full-length $3AB_{1,2,3}CD$ in the absence of $3C^{pro}$ provided *in trans*, as anticipated. The addition of $3C^{pro}$ resulted in the production of smaller proteins due to *trans*-mediated proteolysis of $3AB_{1,2,3}CD$. For the WT precursor, these were predominantly $3AB_{1,2,3}$, 3CD and $3D^{pol}$, in addition to a cluster of $3B_{1,2,3}CD$ precursors, indicative of alternative cleavage pathways. In comparison, the precursor containing the $3B_3^{T>K}$ mutation was processed to $3AB_{1,2,3}$ and 3CD over the duration of the experiment, as observed previously with the active precursor molecule (Figure 2A).

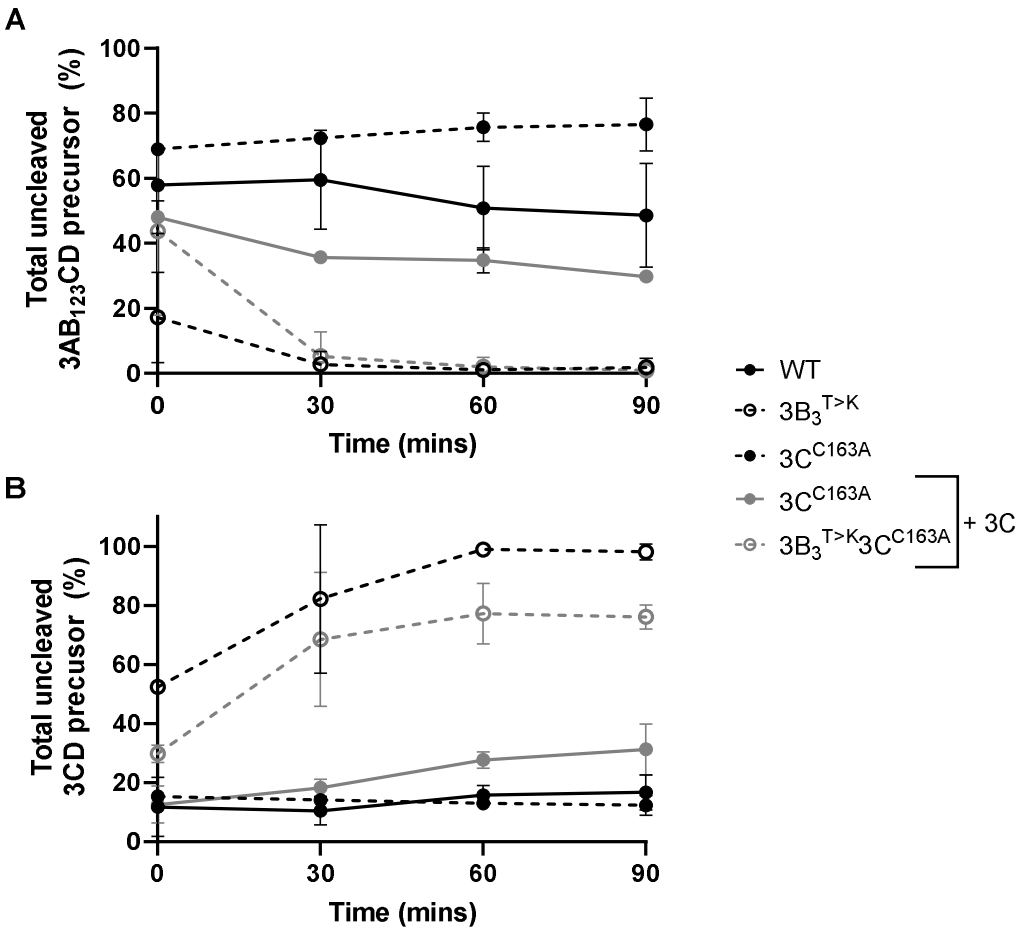

271

272 **Figure 3. The $3B_3^{T>K}$ point mutation drives *trans*-mediated precursor**
273 **proteolysis.** Plasmids expressing proteolytically inactive polyproteins with or without
274 the $3B_3^{T>K}$ mutation (termed $3B_3^{T>K}3C^{C163A}$ and $3C^{C163A}$, respectively) were used to
275 prime coupled [^{35}S] labelled transcription/translation assays, followed by unlabelled
276 amino acid chase. To a duplicate set of reactions 10 µM purified $3C^{pro}$ was added
277 (+3C) immediately after chase. As controls, reactions were setup alongside with the
278 WT or $3B_3^{T>K}$ polyproteins without an inactivated $3C^{pro}$. At regular intervals, samples
279 were taken and reactions stopped by the addition of 2 x Laemmli buffer. Proteins
280 were separated by SDS-PAGE and visualised by autoradiography. The relative
281 proportion of uncleaved $3AB_{1,2,3}CD$ **(A)** or 3CD **(B)** was quantified as a percentage of
282 $3D^{pol}$ containing products (n = 2 ± SD).

To investigate whether the $3B_3^{T>K}$ precursor was also sensitive to cleavage by $3C^{pro}$ when this is present as part of a larger precursor molecule, we generated a $3AB_{1,2,3}CD$ expression construct in which all the cleavage boundaries had been mutated. Thus, the protease activity of this precursor was retained but only in the context of a full-length $3AB_{1,2,3}CD$ polyprotein. Our *trans*-cleavage assay was repeated using this new construct, termed $3AB_{1,2,3}C^{pro}D$, in place of the purified $3C^{pro}$ enzyme used above (Figure 4 and Figure S2).

As before, the $3C^{C163A}$ mutation prevented self-proteolysis when present within the WT precursor or the precursor containing the $3B_3^{T>K}$ substitution, as expected. Addition of the proteolytically active $3AB_{1,2,3}C^{pro}D$ construct resulted in processing of the proteolytically inactive $3AB_{1,2,3}CD$ precursor bearing the $3B_3^{T>K}$ mutation to generate $3AB_{1,2,3}$ and 3CD. This pattern of processing was similar to that observed following addition of active $3C^{pro}$, as observed above (Figure 3). This contrasts with the WT proteolytically inactive $3AB_{1,2,3}CD$ precursor, which was not significantly processed *in trans* by $3AB_{1,2,3}C^{pro}D$. Taken together, these data suggest that the $3B_3^{T>K}$ mutation at the $3B_3$-3C junction generates a cleavage boundary that is preferentially recognised by $3C^{pro}$ (even when delivered as part of a larger precursor). Thus, driving rapid *trans*-mediated proteolysis at this junction results in over-production of a specific set of viral precursor proteins.

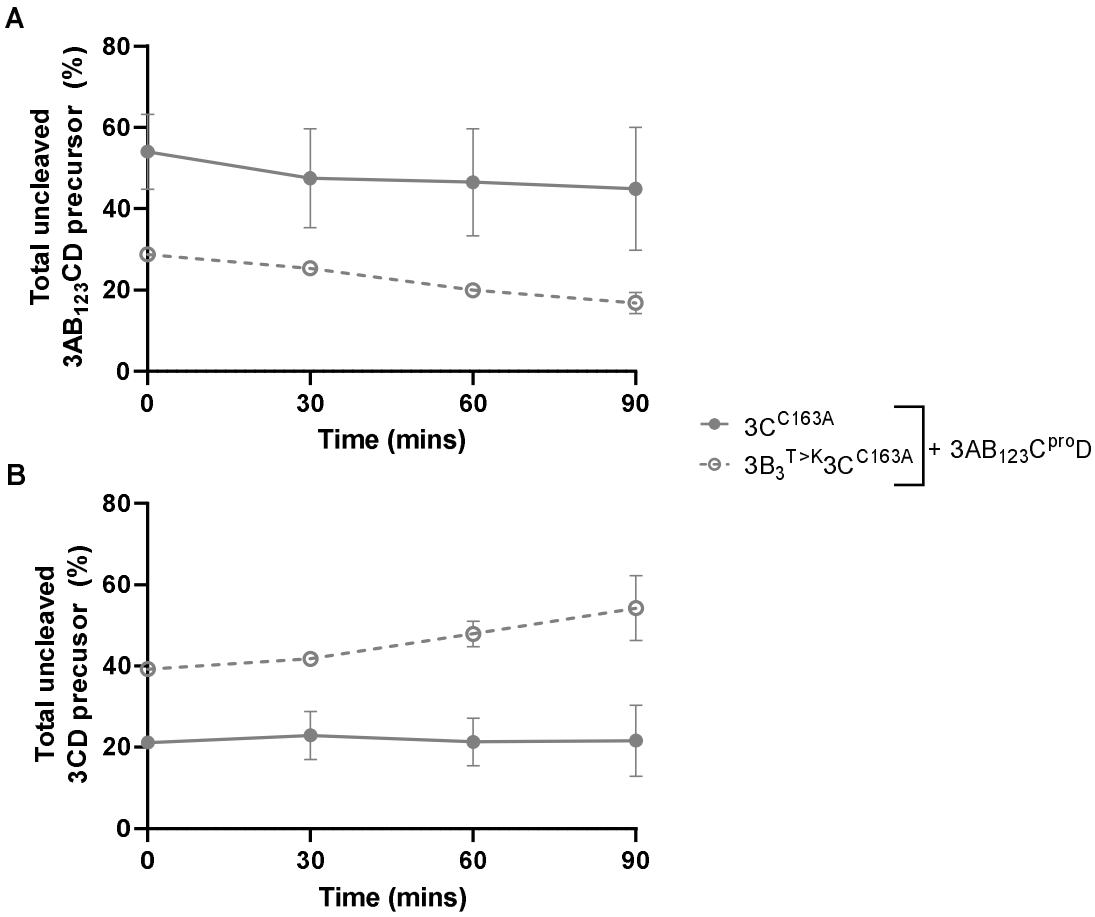

Figure 4. The $3B_3^{T>K}$ point mutation drives *trans*-mediated precursor proteolysis. Plasmids expressing proteolytically inactive versions of WT or $3B_3^{T>K}$ polyproteins ($3C^{C163A}$ and $3B_3^{T>K}3C^{C163A}$, respectively) were used to prime coupled [^{35}S] labelled transcription/translation assays in the presence of $3AB_{1,2,3}C^{pro}D$, a proteolytically active precursor with all cleavage boundaries mutated to prevent self-proteolysis (+$3AB_{123}C^{pro}D$). At regular intervals, samples were taken and reactions stopped by the addition of 2 x Laemmli buffer. Proteins were separated by SDS-PAGE and visualised by autoradiography. The relative proportion of uncleaved $3AB_{1,2,3}CD$ **(A)** or 3CD **(B)** was quantified as a percentage of $3D^{pol}$ containing products (n = 2 ± SD).

Increasing the rate of $3B_3$-3C cleavage prevents production of *trans*-functional 2C and $3D^{pol}$ but not 3B.

The *in vitro* polyprotein processing data above implies that the $3B_3^{T>K}$ mutation increases the rate of proteolysis at the $3B_3$-3C junction by stimulating *trans*-mediated proteolysis. In doing so, it drives the formation of 2BC, $3AB_{1,2,3}$ and 3CD precursors to the detriment of other products such as the enzymes 2C and $3D^{pol}$. In our previous studies we used *trans*-complementation assays to investigate protein function. These assays involve the co-transfection of two replication defective replicon constructs that express different fluorescent reporter genes, allowing their replication to be differentially monitored. Co-transfection of the two replicons allows exchange of viral non-structural proteins within replication complexes to permit replication of one (or both) of the input genomes (41) (Figure 5A). Here, we used this approach to investigate whether stimulating *trans*-mediated proteolysis at the $3B_3$-3C junction prevented the production of functional 2C. To do this, mutants introduced into 2C were investigated to determine if these could be compensated by a replicon harbouring a $3B_3^{T>K}$ mutation. If this is possible, it would indicate that changing the temporal order of polyprotein processing does not prevent 2C function.

To this end, replication-defective mCherry constructs were generated which contained inactivating mutations at catalytic 2C residues (termed, mCherry-$2C^{GK>AA}$) (42). This construct was co-transfected with the ptGFP-$3B_3^{T>K}$ replicon (as used in Figure 1C), or a WT ptGFP replicon control. As a positive control, co-transfections were also performed with an mCherry-$3B_{1,2,3}^{Y3F}$ replicon (which contains inactivating point mutations to the triptych of 3B genes), which we have shown can be complemented *in trans* (16). Co-transfections were also performed with WT mCherry or ptGFP replicons to eliminate the possibility of any dominant-negative effects and

yeast tRNA to act as a negative control for no complementation (Figure 5A). Replication was monitored by both ptGFP and mCherry expression and the number of fluorescent positive cells quantified at 8 hours post-transfection, as documented previously (41). For brevity the key data sets and controls are shown (Figure 5B and 5C) with the complete data set shown in supplementary material (Figure S3).

Replication of the WT mCherry or ptGFP replicon did not significantly change upon co-transfection with any of the RNAs tested, suggestive of no dominant negative effects. Replication of the mCherry-$3B_{1,2,3}^{Y3F}$ replicon was significantly enhanced by the ptGFP-$3B_3^{T>K}$ construct, as anticipated. The mCherry-$2C^{GK>AA}$ replicon was not recovered by any of the helper replicons, suggesting the functions of 2C cannot be provided *in trans* (Figure 5C). We also noticed that no functional complementation was provided to the ptGFP-$3B3^{T>K}$ mutant replicon by co-transfection with mCherry-$3B_{1,2,3}^{Y3F}$. To investigate this further we extended our complementation experiments to include mCherry replicons containing mutations to *cis*-acting RNA replication elements such as the S-fragment or *cre*. The rationale here was that previous studies have demonstrated that deleting *cis*-acting replication elements can improve or allow recovery of replicons *in trans* (41), presumably by increasing the free pool of proteins which would otherwise be sequestered by *cis* interactions. When the ptGFP-$3B_3^{T>K}$ replicon was co-transfected with a mCherry-ΔS or mCherry-*cre*^{A1G} replicon we observed a significance increase in ptGFP expression, indicating that inactivation of these *cis*-acting replication elements permitted complementation of the ptGFP-$3B_3^{T>K}$ replicon in *trans* (Figure 5B). Together this data suggests that the ptGFP-$3B_3^{T>K}$ replicon can supply material *in trans* to recover replicons defective in 3B but not 2C or $3D^{pol}$ and can only receive complementation *in trans* from replicons with inactivating mutations or deletions to *cis*-acting RNA elements.

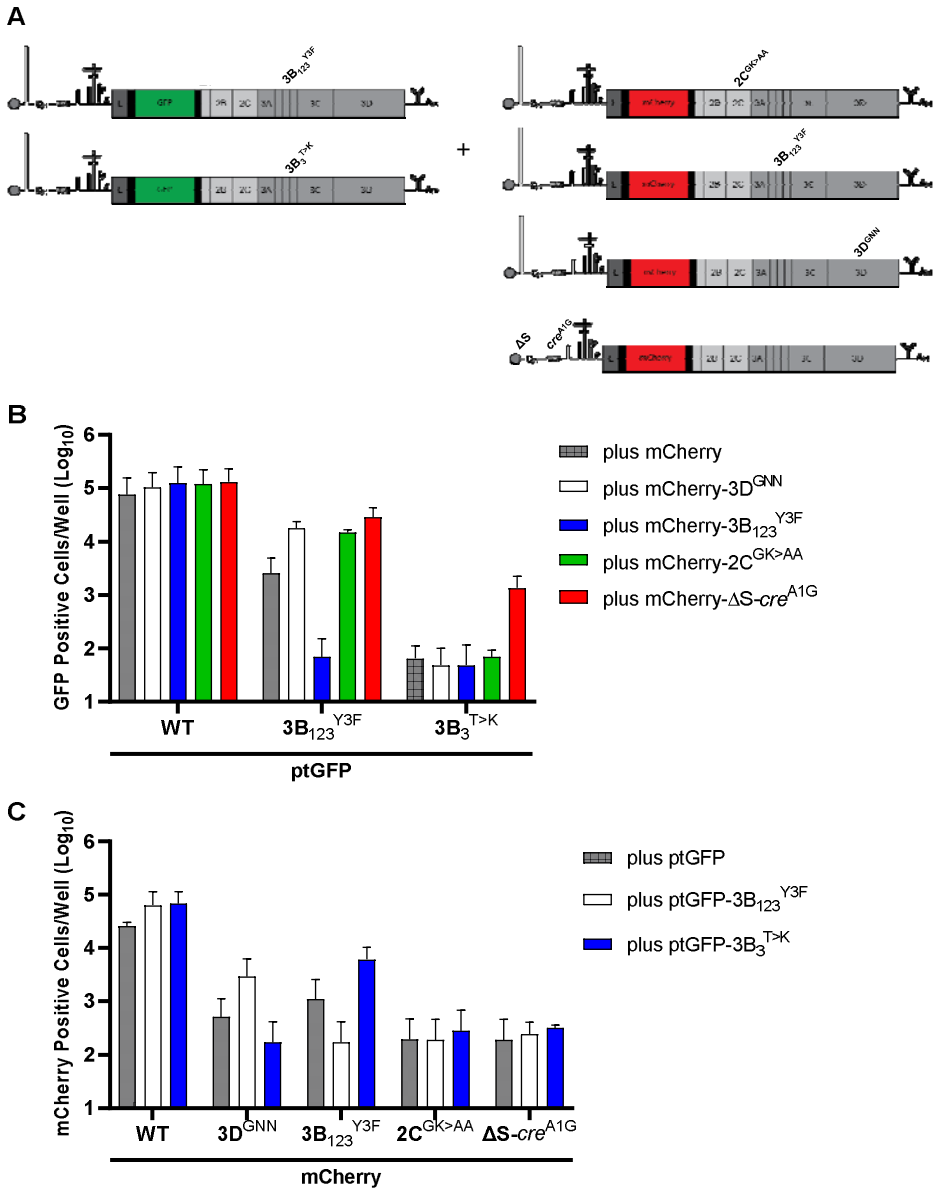

Figure 5. The $3B_3^{T>K}$ substitution prevents complementation of 2C mutants *in trans*. (A) Schematic of the *trans*-complementation experiment which involved co-transfecting BHK-21 cells with mCherry replicons containing replication-defective 2C or 3B mutations together with a WT ptGFP, ptGFP-$3B_3^{T>K}$ or ptGFP-$3D^{GNN}$ replicon. Fluorescent protein expression was monitored hourly for 24 hours. The data show **(B)** ptGFP positive cells per well or **(C)** mCherry positive cells per well at 8 hours post-transfection (n = 2 ± SD).

Complementation of replicons with the $3B_3^{T>K}$ substitution reveals a requirement for the full-length polyprotein.

Having shown that deletion of *cis*-acting RNA elements allowed complementation of the ptGFP-$3B_3^{T>K}$ replicon, we took advantage of this system to identify which protein component was required for complementation. To this end, we generated a new panel of mCherry replicons in which both the S-fragment and *cre* were inactivated but which expressed just a subset of the polyprotein, namely $3AB_{1,2,3}CD$, $3B_{1,2,3}CD$, 3CD or $3D^{pol}$ (Figure 6A). With these constructs, we were able to probe whether the ptGFP-$3B_3^{T>K}$ replicon is missing one of these protein components to initiate replication. This new panel of replicons was used in complementation assays with the same controls as described above, with replication monitored by both ptGFP and mCherry expression, and the number of fluorescent positive cells quantified at 8 hours post-transfection. Again, for clarity the key data sets and controls are shown (Figure 6B and 6C) with the complete data set shown in supplementary material (Figure S4).

As described above we found that replicons lacking a functional S-fragment and/or *cre*, were able to significantly increase the replication of the ptGFP-$3B_3^{T>K}$ replicon, with ptGFP expression increasing >10-fold compared to the controls. In contrast, no complementation of the ptGFP-$3B_3^{T>K}$ replicon was observed when co-transfected with RNAs expressing just $3AB_{1,2,3}CD$, $3B_{1,2,3}CD$, 3CD or $3D^{pol}$. Hence it would appear that $3AB_{1,2,3}CD$ is not sufficient to support replication of a $3B_3^{T>K}$ replicon and provision of 2BC containing proteins is also required.

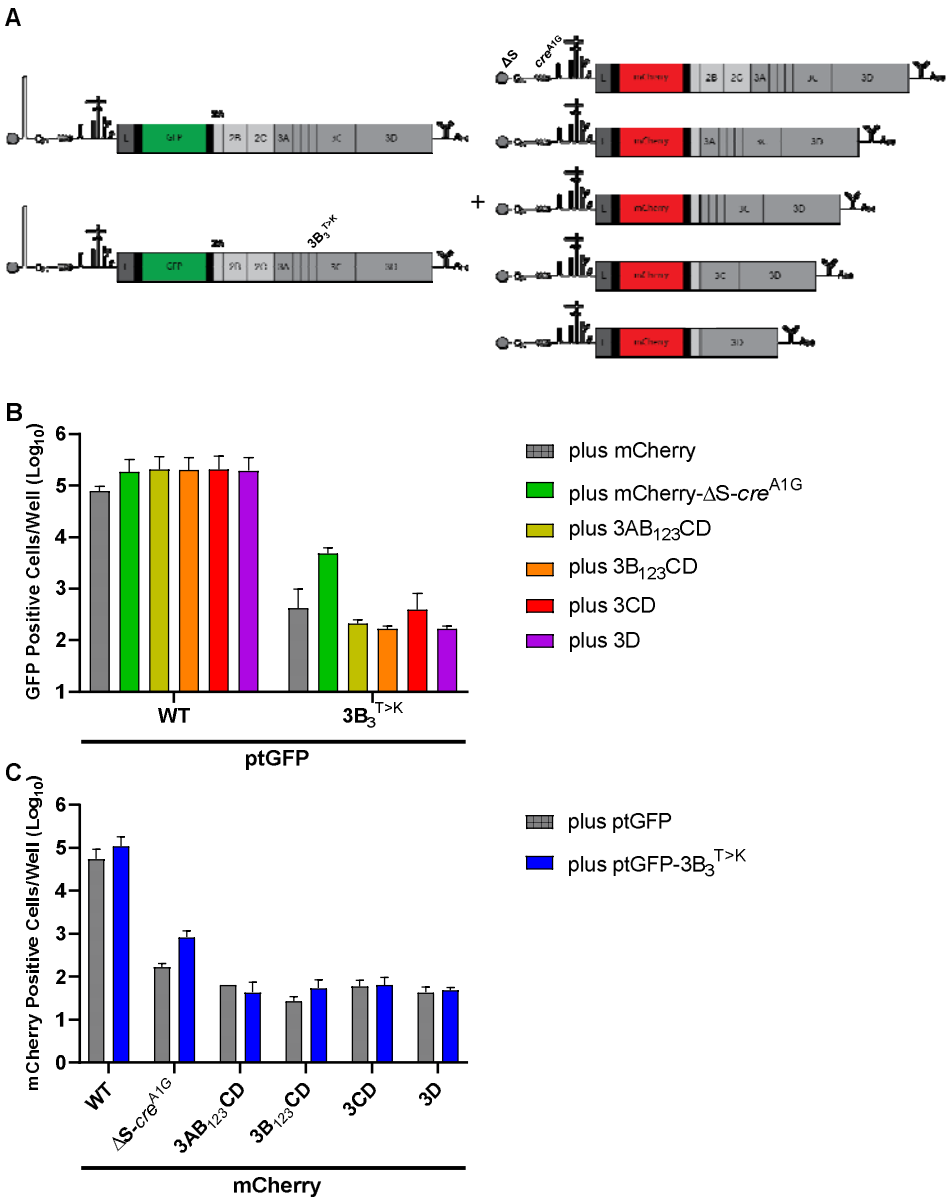

Figure 6. S-fragment deletions allow *trans*-complementation of *cis*-acting replication components. (A) Schematic of the trans-complementation experiment which involved co-transfecting BHK-21 cells with mCherry replicons containing S-fragment deletions together with a WT ptGFP, ptGFP-$3B_3^{T>K}$ or ptGFP-$3D^{GNN}$ replicon. Fluorescent protein expression was monitored hourly for 24 hours. The data show **(B)** ptGFP positive cells per well or **(C)** mCherry positive cells per well at 8 hours post-transfection (n = 2 ± SD).

The $3B_3^{T>K}$ mutation does not prevent RNA-protein interactions.

A key observation from our *trans*-complementation work is that the $3B_3^{T>K}$ mutation prevents complementation of this non-functional replicon unless the *cis*-acting S-fragment or *cre* elements are deleted from the helper RNA. A possible explanation is that the altered cleavage pattern induced by the $3B_3^{T>K}$ mutation prevents replication components (e.g., the 2C helicase or $3D^{pol}$) from interacting with the template RNA, thus preventing its replication.

To investigate this possibility, we adapted a proximity ligation assay (PLA) to study interactions between replicon RNA and components of the replication complex. Firstly, we *in vitro* transcribed ptGFP-$3B_3^{T>K}$ replicon RNA (or ptGFP-$3D^{GNN}$ and ptGFP-$3B_{1,2,3}^{Y3F}$ controls) in the presence of BrUTP to generate BrU labelled replicon RNA. Alongside, a WT ptGFP was transcribed with BrUTP and used to confirm that BrU labelling had no significant inhibitory effect on replicon replication (data unincluded). The ptGFP-$3B_3^{T>K}$ BrU replicon was co-transfected into BHK-21 cells seeded on coverslips together with a WT replicon in which $3D^{pol}$ had been labelled with a HA epitope (termed $3D^{HA}$). We have previously demonstrated that tagging $3D^{pol}$ with HA in this manner does not affect replication (41). The coverslips were fixed and the interaction between the BrU-$3B_3^{T>K}$ RNA and $3D^{HA}$ probed by PLA using anti-BrU and anti-HA antibodies. This allows RNA-protein interactions between the ptGFP-BrU-$3B_3^{T>K}$ RNA and $3D^{HA}$ protein to be measured *in situ*. A positive PLA signal indicates that the mutant replicon RNA can associate with enzymes of the replication complex provided *in trans*. No signal indicates a lack of association (Figure 7).

Co-transfection of the WT ptGFP BrU labelled replicon with the WT $3D^{HA}$ replicon generated PLA signals that were easily detectable, indicative of interactions between

the ptGFP RNA and $3D^{HA}$ protein as predicted from mixing of replication complex components. In contrast, little or no PLA signal was detected when a WT BrU labelled poliovirus replicon (BrU-PV) was co-transfected with the $3D^{HA}$ helper replicon, suggesting the PLA signal is generated through specific mixing of replication complexes. Co-transfection of the ptGFP-$3B_3^{T>K}$, ptGFP-$3B_{1,2,3}^{Y3F}$ or ptGFP-$3D^{GNN}$ BrU labelled replicon RNAs with the WT $3D^{HA}$ replicon also generated PLA signals that were easily detectable, albeit at a lower level than in the control sample. This would suggest the $3B_3^{T>K}$ mutation does not prevent recruitment of its cognate RNA with a functional RNA polymerase.

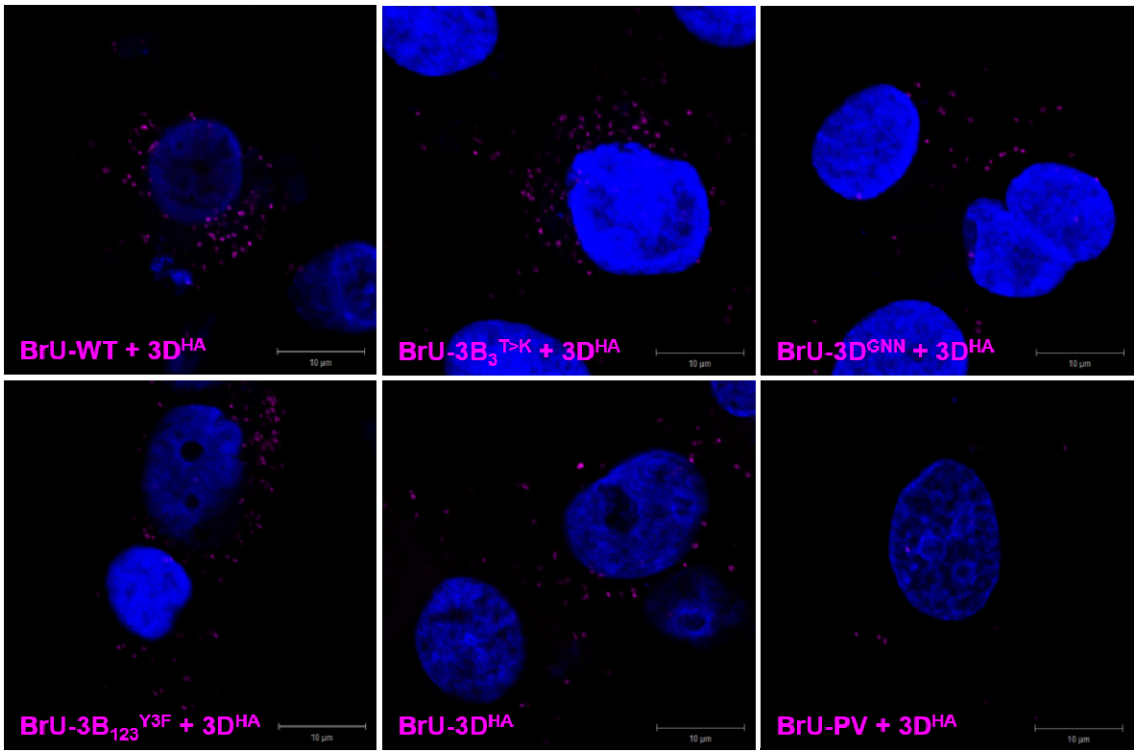

Figure 7. Detection of FMDV RNA-protein complexes by PLA. BHK-21 cells were co-transfected with BrU-labelled ptGFP replicon RNA together with $3D^{HA}$-labelled replicon RNA. At 4 hours post-transfection cells were fixed and $3D^{HA}$-BrU RNA complexes detected by proximity ligation assay (PLA) using anti-HA and anti-BrU primary antibodies together with PLA-labelled secondary antibodies. The *in-situ* PLA signal is detected as foci in the cell cytoplasm (pseudo-coloured magenta). Cell nuclei were stained with DAPI (pseudo-coloured blue). Images were captured on a Zeiss LSM-880 confocal microscope (bar 10 µm).

Discussion

All well-studied positive-sense RNA viruses produce polyproteins that help compensate for a relatively limited coding capacity. These polyproteins are processed by viral protease(s) to generate mature proteins via functional intermediates in a highly regulated manner that modulates viral replication. However, establishing how polyprotein processing regulates viral replication can be challenging due to the intricate nature of these interactions. In a previous study of the FMDV polyprotein we showed that changing six amino acids at the $3B_3$-3C cleavage junction prevents viral replication by disrupting polyprotein processing (16). We postulated that this observation provided an opportunity to investigate the role of FMDV polyproteins in viral genome replication. First we investigated whether consequences of substituting the six amino acids could be replicated by a single change. To do this we targeted the P2 residue at the $3B_3$-3C cleavage junction, which from our previous mutational investigation appeared to be the most important for dictating cleavage efficiency. A single lysine substitution was introduced in this position, which we predicted would increase processing and prevent replication. Using a GFP encoding replicon, we showed this single substitution ($3B_3^{T>K}$) prevented viral replication and in *in vitro* translation assays changed polyprotein processing, as predicted.

To build a more complete picture of how the $3B_3^{T>K}$ construct changed polyprotein processing and understand the mechanism that underpinned this change, we employed a combination of *in vitro* translation assays, immunoprecipitation and *trans*-cleavage assays in the context of the FMDV non-structural polyprotein. We found that a $3B_3$-3C cleavage junction bearing this mutation was more efficiently cleaved by $3C^{pro}$ *in trans* compared to WT. Furthermore, the $3B_3^{T>K}$ substitution also

rendered this cleavage junction sensitive to proteolysis by $3C^{pro}$ when the protease was present as part of a larger precursor (i.e., as part of another molecule of $3AB_{1,2,3}CD$). Thus, the consequence of introducing the $3B_3^{T>K}$ substitution was to generate a substrate that was more efficiently cleaved (potentially equal to or greater than either 2B-2C or 2C-3A cleavage sites). This changes the subset of proteins produced; generating $2BC3AB_{1,2,3}$ (that is not typically observed during infection (7, 43)) significantly increasing levels of 3CD and 2BC and reducing levels of the $3AB_{1,2,3}CD$. The identity of these products was based on both molecular weight and immunoprecipitation experiments. The $3B_3^{T>K}$ mutant construct did generate fully-cleaved 2B and 2C at a reduced rate demonstrating that $3C^{pro}$ as part of 3CD is proteolytically active, but processing of $3AB_{1,2,3}$ and 3CD was severely impaired as observed previously (16).

Our data are consistent with biochemical investigations using purified $3C^{pro}$ which showed that charged residues in the P2 position of the cleavage junction are more efficiently recognised (40, 44-46). It is also consistent with the suggestion that $3C^{pro}$ retains activity as part of a larger precursor but potentially at lower efficiencies (47-50). Our data therefore agrees with a mechanism of polyprotein processing (suggested from studies with other picornaviruses) in which $3C^{pro}$ as part of a larger precursor can process the WT 2B-2C and/or 2C-3A junctions most efficiently *in trans*, hence providing a level of regulation to the processing cascade. After these initial cleavage events, $3AB_{1,2,3}CD$ is processed more slowly to allow intermediate and mature cleavage products to fulfil their roles in viral replication (37). Processing of the $3AB_{1,2,3}CD$ precursor can thus proceed potentially through both *cis* and *trans* mechanisms (i.e., intra- and inter-molecular cleavage) and can give rise to alternative precursors, for example, $3AB_{1,2,3}C$ and 3CD. It is clearly suggested from

our data that *trans* cleavage of one $3AB_{1,2,3}CD$ molecule by another polyprotein is possible. However, the WT precursor was not processed efficiently by $3AB_{1,2,3}CD$ *in trans*, and the observation that $3C^{pro}$ in the context of 3CD is proteolytically active, but only able to cleave efficiently at 2B-2C and 2C-3A junctions could suggest that other factors (e.g., a *cis* mediated mechanism), are also involved. Picornavirus $3C^{pro}$ proteins are also implicated in RNA binding and lipid biogenesis (potentially as part of a precursor), and therefore may act as co-factors to dictate processing pathways (30, 51, 52).

Using *trans*-complementation assays we investigated the function of these different sets of precursors in FMDV replication. A replicon containing the $3B_3^{T>K}$ substitution (i.e., producing increased level of 2BC, $3AB_{1,2,3}$ and 3CD), was able to complement defective mutations in the 3B proteins but not 2C or $3D^{pol}$, suggesting that this replicon can produce active primers for replication, $3B_1$, $3B_2$, and/or $3B_3$ but inactive replication enzymes, $2C^{pro}$ and $3D^{pol}$. Interestingly the $3B_3^{T>K}$ replicon was only complemented by a replicon lacking *cis*-acting RNA replication elements (*cre*, S-fragment or both) and when the protein components were provided as part of an entire polyprotein. One interpretation of these pieces of data is that a functional interaction between the non-structural polyprotein and viral RNA elements is required to generate functional enzymes for replication (e.g., $2C^{pro}$ and $3D^{pol}$ but not 3B). Hence, if processing of the precursor occurs too rapidly it cannot associate with these RNA elements required for replication and could provide a level of temporal control. A similar mechanism has been suggested for PV where two molecules of 3ABCD are required for replication, one which produces 3CD that interacts with viral RNA structures while one produces enzymatically active $3D^{pol}$ (33, 37, 53, 54). This two molecule model of processing of 3ABCD required for replication would also be

compatible with data that suggests that a larger precursor (such as 3BC) is required to deliver 3B for RNA replication (15, 55, 56). This work extends the growing body of evidence suggesting that processing intermediates are essential for controlling temporally and structurally the organisation of the picornavirus replication organelle.

Materials and Methods

Cell lines and plasmids

BHK-21 cells obtained from the ATCC (LGC Standard) were maintained in Dulbecco's modified Eagle's medium with glutamine (Sigma-Aldrich) supplemented with 10 % FCS, 50 U / mL penicillin and 50 µg / mL streptomycin.

Plasmids carrying wild-type FMDV replicons, pRep-mCherry and pRep-ptGFP, have already been described (39, 57), along with equivalent plasmids containing $3D^{GNN}$, $3B_{3/2}$ and ΔS-fragment mutations (16, 39, 41). Mutations within these plasmids were performed by standard two-step overlapping PCR mutagenesis. For coupled *in vitro* transcription and translation experiments pcDNA3.1(+) based expression plasmids were generated by PCR. Briefly, the relevant FMDV sequence was amplified to including flanking *Not*I restriction enzymes and upstream Kozak modified translational start site. The *Not*I digested PCR products were cloned into *Not*I digested pcDNA3.1(+) (Thermo Fisher Scientific). The sequence of all plasmids used in this study was confirmed by Sanger sequencing. The sequences of all primers and plasmids are available on request.

Coupled transcription and translation reactions

Coupled *in vitro* transcription and translation assays were performed using the TNT Quick Coupled Transcription/Translation system (Promega) as described previously (16). Reactions contained 10 µL lysate with 250 ng of pcDNA T7 expression plasmid and 0.5 µL [^{35}S] methionine/cysteine (PerkinElmer). Reactions were incubated at 30ºC for 40 minutes chasing with 2 µL of 50 mg / mL unlabelled methionine/cysteine. Reactions were stopped at 20 minute or hourly intervals by the addition of 2 x Laemmli buffer. Samples were separated by SDS-PAGE before visualisation of radiolabelled products by autoradiography.

For the *trans*-cleavage assays, the TNT reactions were supplemented with purified FMDV $3C^{pro}$ (a kind gift from Dr Tobias Tuthill (58)) to the indicated final concentration from dilution of a 1 mM stock, simultaneous to the addition of unlabelled methionine/cysteine. Reactions were stopped at 20 minute or hourly intervals by the addition of 2 x Laemmli buffer and the $3C^{pro}$-mediated proteolysis of radiolabelled precursor monitored by SDS-PAGE.

In vitro transcription

Plasmids containing cDNA copies of FMDV replicons were linearised with *Asc*I before being used to generate T7 *in vitro* transcribed RNA as previously described (39, 41). The reaction was incubated at 32ºC for 4 hours before being treated with DNase for 20 minutes at 37ºC then purified using an RNA clean and concentrate kit (Zymo Research). The RNA quality was checked using a MOPS/formaldehyde agarose gel electrophoresis.

Replication and complementation assays

BHK-21 cells were seeded into 24-well tissue cultures vessels, allowed to adhere overnight for 16 hours, before duplicate wells were transfected with 1 µg of each *in vitro* transcribed RNA using Lipofectin (Thermo Fisher Scientific) as previously described (39). For co-transfection complementation assays 500 ng of each RNA molecules were mixed prior to the addition of Lipofectin reagent as previously described (41). Fluorescent reporter expression was monitored using an IncuCyte Zoom Dual Colour FLR (Essen BioSciences) live-cell imaging system housed within a humidified incubator scanning hourly up to 24 hours post-transfection. Images were captured and analysed using the associated software for fluorescent protein expression, as previously described (41). Control transfections (untransfected and the $3D^{GNN}$ transfection for input translation) were used to determine fluorescent

thresholds and identify positive objects from background fluorescence. A positive object was determined as having an average fluorescent intensity of >8 green calibration units (GCU; an arbitrary fluorescent unit) and >2 RCU (red calibration units), which were kept constant throughout the experiments. The number of positive cells per well was determined from the average of up to nine non-overlapping images per well. Unless stated otherwise, data are presented as mean fluorescent positive cells per well at 8 hours post-transfection when replication was approximately maximal. For each experiment, the data were analysed as both fluorescent cell counts per well and total fluorescent intensity per well. There was no difference observed when the data were analysed in either way. Unless otherwise stated, statistical analysis was performed using a two-tailed unpaired t-test.

Immunofluorescence and proximity ligation assays (PLA)

BHK-21 cells seeded onto coverslips were co-transfected with replicon RNA before fixing in 4 % paraformaldehyde and washing with PBS. Immunofluorescence was conducted as previously described (41). Primary antibodies used were sheep anti-BrdU (Sigma-Aldrich), rabbit anti-FMDV 3D (a kind gift from Francisco Sobrino) and mouse anti-HA (Sigma-Aldrich). Proximity ligation assays (PLA) were conducted using the Duolink® In Situ Red Kit (Sigma-Aldrich), following manufacturer's instructions.

Immunoprecipitation

Immunoprecipitation reactions were performed using Dynabeads Protein G (Invitrogen). To bind the antibody to magnetic beads, 5 µL of the FMDV 2C antibody (a kind gift from Francisco Sobrino) was mixed with 195 µL PBS and incubated at room temperature with 50 µL magnetic beads, shaking for 1 hour, after which the supernatant was removed from the beads. Transcription and translation reaction

samples were mixed with 200 µL PBS and incubated shaking at room temperature with 25 µL of Dynabeads as a pre-clear step. The tube was placed on the magnet and the supernatant removed. This was added to the 50 µL of Dynabeads with the 2C antibody bound and incubated at room temperature shaking for 1 hour. The flow through was removed and added to 2x Laemmli buffer. The beads were washed three times with PBS pH 7.4 with 0.02 % Tween 20 and each wash supernatant retained. Proteins were eluted from the beads by adding 50 µL of 2x Laemmli buffer and heating to 100ºC.

606 **Funding**

607 This work was supported by BBSRC grant (BB/T015748/1) awarded to MRH, DJR
608 and NJS. DMP was funded by a BBSRC DTP studentship (BB/M011151/1). MRH
609 was also supported by the MRC (MR/S007229/1). The funders had no role in the
610 study design, data collection and analysis, decision to publish or preparation of the
611 manuscript.

612 **Acknowledgements**

613 We thank Francisco Sobrino (Centro De Biologia Molecular Severo Ochoa, Madrid)
614 for the gift of FMDV primary antibodies and Toby Tuthill (The Pirbright Institute,
615 Pirbright) for the gift of purified 3C.

616 **Author contributions**

617 MRH, NJS and DJR designed the study and wrote the manuscript. DMP conducted
618 the *in vitro* translation experiments. DMP and MRH conducted the replication assays.
619 MRH conducted the immunofluorescence assays. DMP and MRH analysed the data.
620 MRH, NJS and DJR provided supervision.

621 **Materials & correspondence**

622 Correspondence and materials requests should be directed to MRH.

References

1. Yost SA, Marcotrigiano J. 2013. Viral precursor polyproteins: keys of regulation from replication to maturation. Curr Opin Virol 3:137-42.
2. Moffat K, Knox C, Howell G, Clark SJ, Yang H, Belsham GJ, Ryan M, Wileman T. 2007. Inhibition of the secretory pathway by foot-and-mouth disease virus 2BC protein is reproduced by coexpression of 2B with 2C, and the site of inhibition is determined by the subcellular location of 2C. J Virol 81:1129-39.
3. Zhu Z, Wang G, Yang F, Cao W, Mao R, Du X, Zhang X, Li C, Li D, Zhang K, Shu H, Liu X, Zheng H. 2016. Foot-and-Mouth Disease Virus Viroporin 2B Antagonizes RIG-I-Mediated Antiviral Effects by Inhibition of Its Protein Expression. J Virol 90:11106-11121.
4. Sweeney TR, Cisnetto V, Bose D, Bailey M, Wilson JR, Zhang X, Belsham GJ, Curry S. 2010. Foot-and-mouth disease virus 2C is a hexameric AAA+ protein with a coordinated ATP hydrolysis mechanism. J Biol Chem 285:24347-59.
5. Carrillo C, Tulman ER, Delhon G, Lu Z, Carreno A, Vagnozzi A, Kutish GF, Rock DL. 2005. Comparative genomics of foot-and-mouth disease virus. J Virol 79:6487-504.
6. Roberts PJ, Belsham GJ. 1995. Identification of critical amino acids within the foot-and-mouth disease virus leader protein, a cysteine protease. Virology 213:140-6.
7. Vakharia VN, Devaney MA, Moore DM, Dunn JJ, Grubman MJ. 1987. Proteolytic processing of foot-and-mouth disease virus polyproteins expressed in a cell-free system from clone-derived transcripts. J Virol 61:3199-207.

8. Strebel K, Beck E. 1986. A second protease of foot-and-mouth disease virus. J Virol 58:893-9.

9. Donnelly MLL, Luke G, Mehrotra A, Li X, Hughes LE, Gani D, Ryan MD. 2001. Analysis of the aphthovirus 2A/2B polyprotein 'cleavage' mechanism indicates not a proteolytic reaction, but a novel translational effect: a putative ribosomal 'skip'. J Gen Virol 82:1013-1025.

10. Kitamura N, Semler BL, Rothberg PG, Larsen GR, Adler CJ, Dorner AJ, Emini EA, Hanecak R, Lee JJ, van der Werf S, Anderson CW, Wimmer E. 1981. Primary structure, gene organization and polypeptide expression of poliovirus RNA. Nature 291:547-53.

11. Pallansch MA, Kew OM, Semler BL, Omilianowski DR, Anderson CW, Wimmer E, Rueckert RR. 1984. Protein processing map of poliovirus. J Virol 49:873-80.

12. Gao Y, Sun SQ, Guo HC. 2016. Biological function of Foot-and-mouth disease virus non-structural proteins and non-coding elements. Virol J 13:107.

13. Grubman MJ, Baxt B. 2004. Foot-and-mouth disease. Clin Microbiol Rev 17:465-93.

14. Bedard KM, Semler BL. 2004. Regulation of picornavirus gene expression. Microbes Infect 6:702-13.

15. Oh HS, Pathak HB, Goodfellow IG, Arnold JJ, Cameron CE. 2009. Insight into poliovirus genome replication and encapsidation obtained from studies of 3B-3C cleavage site mutants. J Virol 83:9370-87.

16. Herod MR, Gold S, Lasecka-Dykes L, Wright C, Ward JC, McLean TC, Forrest S, Jackson T, Tuthill TJ, Rowlands DJ, Stonehouse NJ. 2017. Genetic

672 economy in picornaviruses: Foot-and-mouth disease virus replication exploits
673 alternative precursor cleavage pathways. PLoS Pathog 13:e1006666.
674 17. Oh HS, Banerjee S, Aponte-Diaz D, Sharma SD, Aligo J, Lodeiro MF, Ning G,
675 Sharma R, Arnold JJ, Cameron CE. 2018. Multiple poliovirus-induced
676 organelles suggested by comparison of spatiotemporal dynamics of
677 membranous structures and phosphoinositides. PLoS Pathog 14:e1007036.
678 18. den Boon JA, Ahlquist P. 2010. Organelle-like membrane
679 compartmentalization of positive-strand RNA virus replication factories. Annu
680 Rev Microbiol 64:241-56.
681 19. Belsham GJ, Brangwyn JK. 1990. A region of the 5' noncoding region of foot-
682 and-mouth disease virus RNA directs efficient internal initiation of protein
683 synthesis within cells: involvement with the role of L protease in translational
684 control. J Virol 64:5389-95.
685 20. Lopez de Quinto S, Martinez-Salas E. 1997. Conserved structural motifs
686 located in distal loops of aphthovirus internal ribosome entry site domain 3 are
687 required for internal initiation of translation. J Virol 71:4171-5.
688 21. Lopez de Quinto S, Saiz M, de la Morena D, Sobrino F, Martinez-Salas E.
689 2002. IRES-driven translation is stimulated separately by the FMDV 3'-NCR
690 and poly(A) sequences. Nucleic Acids Res 30:4398-405.
691 22. Mason PW, Bezborodova SV, Henry TM. 2002. Identification and
692 characterization of a cis-acting replication element (cre) adjacent to the
693 internal ribosome entry site of foot-and-mouth disease virus. J Virol 76:9686-
694 94.
695 23. Forss S, Schaller H. 1982. A tandem repeat gene in a picornavirus. Nucleic
696 Acids Res 10:6441-50.

697 24. Paul AV, Peters J, Mugavero J, Yin J, van Boom JH, Wimmer E. 2003.
698 Biochemical and genetic studies of the VPg uridylylation reaction catalyzed by
699 the RNA polymerase of poliovirus. J Virol 77:891-904.
700 25. Paul AV, van Boom JH, Filippov D, Wimmer E. 1998. Protein-primed RNA
701 synthesis by purified poliovirus RNA polymerase. Nature 393:280-4.
702 26. Falk MM, Sobrino F, Beck E. 1992. VPg gene amplification correlates with
703 infective particle formation in foot-and-mouth disease virus. J Virol 66:2251-60.
704 27. Paul AV, Rieder E, Kim DW, van Boom JH, Wimmer E. 2000. Identification of
705 an RNA hairpin in poliovirus RNA that serves as the primary template in the in
706 vitro uridylylation of VPg. J Virol 74:10359-70.
707 28. Nayak A, Goodfellow IG, Belsham GJ. 2005. Factors required for the
708 Uridylylation of the foot-and-mouth disease virus 3B1, 3B2, and 3B3 peptides
709 by the RNA-dependent RNA polymerase (3Dpol) in vitro. J Virol 79:7698-706.
710 29. Kloc A, Diaz-San Segundo F, Schafer EA, Rai DK, Kenney M, de Los Santos
711 T, Rieder E. 2017. Foot-and-mouth disease virus 5'-terminal S fragment is
712 required for replication and modulation of the innate immune response in host
713 cells. Virology 512:132-143.
714 30. Amero CD, Arnold JJ, Moustafa IM, Cameron CE, Foster MP. 2008.
715 Identification of the oriI-binding site of poliovirus 3C protein by nuclear
716 magnetic resonance spectroscopy. J Virol 82:4363-70.
717 31. Marcotte LL, Wass AB, Gohara DW, Pathak HB, Arnold JJ, Filman DJ,
718 Cameron CE, Hogle JM. 2007. Crystal structure of poliovirus 3CD protein:
719 virally encoded protease and precursor to the RNA-dependent RNA
720 polymerase. J Virol 81:3583-96.

721 32. Xiang W, Harris KS, Alexander L, Wimmer E. 1995. Interaction between the
722 5'-terminal cloverleaf and 3AB/3CDpro of poliovirus is essential for RNA
723 replication. J Virol 69:3658-67.
724 33. Gamarnik AV, Andino R. 2000. Interactions of viral protein 3CD and poly(rC)
725 binding protein with the 5' untranslated region of the poliovirus genome. J
726 Virol 74:2219-26.
727 34. Harris KS, Xiang W, Alexander L, Lane WS, Paul AV, Wimmer E. 1994.
728 Interaction of poliovirus polypeptide 3CDpro with the 5' and 3' termini of the
729 poliovirus genome. Identification of viral and cellular cofactors needed for
730 efficient binding. J Biol Chem 269:27004-14.
731 35. Parsley TB, Towner JS, Blyn LB, Ehrenfeld E, Semler BL. 1997. Poly (rC)
732 binding protein 2 forms a ternary complex with the 5'-terminal sequences of
733 poliovirus RNA and the viral 3CD proteinase. RNA 3:1124-34.
734 36. Yang Y, Rijnbrand R, Watowich S, Lemon SM. 2004. Genetic evidence for an
735 interaction between a picornaviral cis-acting RNA replication element and
736 3CD protein. J Biol Chem 279:12659-67.
737 37. Spear A, Ogram SA, Morasco BJ, Smerage LE, Flanegan JB. 2015. Viral
738 precursor protein P3 and its processed products perform discrete and
739 essential functions in the poliovirus RNA replication complex. Virology
740 485:492-501.
741 38. Towner JS, Mazanet MM, Semler BL. 1998. Rescue of defective poliovirus
742 RNA replication by 3AB-containing precursor polyproteins. J Virol 72:7191-
743 200.

744 39. Herod MR, Loundras EA, Ward JC, Tulloch F, Rowlands DJ, Stonehouse NJ.
745 2015. Employing transposon mutagenesis to investigate foot-and-mouth
746 disease virus replication. J Gen Virol 96:3507-3518.
747 40. Sweeney TR, Roque-Rosell N, Birtley JR, Leatherbarrow RJ, Curry S. 2007.
748 Structural and mutagenic analysis of foot-and-mouth disease virus 3C
749 protease reveals the role of the beta-ribbon in proteolysis. J Virol 81:115-24.
750 41. Herod MR, Ferrer-Orta C, Loundras EA, Ward JC, Verdaguer N, Rowlands DJ,
751 Stonehouse NJ. 2016. Both cis and trans Activities of Foot-and-Mouth
752 Disease Virus 3D Polymerase Are Essential for Viral RNA Replication. J Virol
753 90:6864-6883.
754 42. Gladue DP, O'Donnell V, Baker-Branstetter R, Holinka LG, Pacheco JM,
755 Fernandez-Sainz I, Lu Z, Brocchi E, Baxt B, Piccone ME, Rodriguez L, Borca
756 MV. 2012. Foot-and-mouth disease virus nonstructural protein 2C interacts
757 with Beclin1, modulating virus replication. J Virol 86:12080-90.
758 43. Clarke BE, Sangar DV. 1988. Processing and assembly of foot-and-mouth
759 disease virus proteins using subgenomic RNA. J Gen Virol 69 (Pt 9):2313-25.
760 44. Birtley JR, Curry S. 2005. Crystallization of foot-and-mouth disease virus 3C
761 protease: surface mutagenesis and a novel crystal-optimization strategy. Acta
762 Crystallogr D Biol Crystallogr 61:646-50.
763 45. Birtley JR, Knox SR, Jaulent AM, Brick P, Leatherbarrow RJ, Curry S. 2005.
764 Crystal structure of foot-and-mouth disease virus 3C protease. New insights
765 into catalytic mechanism and cleavage specificity. J Biol Chem 280:11520-7.
766 46. Zunszain PA, Knox SR, Sweeney TR, Yang J, Roque-Rosell N, Belsham GJ,
767 Leatherbarrow RJ, Curry S. 2010. Insights into cleavage specificity from the

768 crystal structure of foot-and-mouth disease virus 3C protease complexed with
769 a peptide substrate. J Mol Biol 395:375-89.
770 47. Davis GJ, Wang QM, Cox GA, Johnson RB, Wakulchik M, Dotson CA,
771 Villarreal EC. 1997. Expression and purification of recombinant rhinovirus 14
772 3CD proteinase and its comparison to the 3C proteinase. Arch Biochem
773 Biophys 346:125-30.
774 48. Jurgensen D, Kusov YY, Facke M, Krausslich HG, Gauss-Muller V. 1993.
775 Cell-free translation and proteolytic processing of the hepatitis A virus
776 polyprotein. J Gen Virol 74 (Pt 4):677-83.
777 49. Probst C, Jecht M, Gauss-Muller V. 1998. Processing of proteinase
778 precursors and their effect on hepatitis A virus particle formation. J Virol
779 72:8013-20.
780 50. Ypma-Wong MF, Dewalt PG, Johnson VH, Lamb JG, Semler BL. 1988.
781 Protein 3CD is the major poliovirus proteinase responsible for cleavage of the
782 P1 capsid precursor. Virology 166:265-70.
783 51. Banerjee S, Aponte-Diaz D, Yeager C, Sharma SD, Ning G, Oh HS, Han Q,
784 Umeda M, Hara Y, Wang RYL, Cameron CE. 2018. Hijacking of multiple
785 phospholipid biosynthetic pathways and induction of membrane biogenesis by
786 a picornaviral 3CD protein. PLoS Pathog 14:e1007086.
787 52. Shengjuler D, Chan YM, Sun S, Moustafa IM, Li ZL, Gohara DW, Buck M,
788 Cremer PS, Boehr DD, Cameron CE. 2017. The RNA-Binding Site of
789 Poliovirus 3C Protein Doubles as a Phosphoinositide-Binding Domain.
790 Structure 25:1875-1886 e7.
791 53. Toyoda H, Franco D, Fujita K, Paul AV, Wimmer E. 2007. Replication of
792 poliovirus requires binding of the poly(rC) binding protein to the cloverleaf as

well as to the adjacent C-rich spacer sequence between the cloverleaf and the internal ribosomal entry site. J Virol 81:10017-28.

54. Shen M, Reitman ZJ, Zhao Y, Moustafa I, Wang Q, Arnold JJ, Pathak HB, Cameron CE. 2008. Picornavirus genome replication. Identification of the surface of the poliovirus (PV) 3C dimer that interacts with PV 3Dpol during VPg uridylylation and construction of a structural model for the PV 3C2-3Dpol complex. J Biol Chem 283:875-88.

55. Pathak HB, Oh HS, Goodfellow IG, Arnold JJ, Cameron CE. 2008. Picornavirus genome replication: roles of precursor proteins and rate-limiting steps in oriI-dependent VPg uridylylation. J Biol Chem 283:30677-88.

56. Nayak A, Goodfellow IG, Woolaway KE, Birtley J, Curry S, Belsham GJ. 2006. Role of RNA structure and RNA binding activity of foot-and-mouth disease virus 3C protein in VPg uridylylation and virus replication. J Virol 80:9865-75.

57. Tulloch F, Pathania U, Luke GA, Nicholson J, Stonehouse NJ, Rowlands DJ, Jackson T, Tuthill T, Haas J, Lamond AI, Ryan MD. 2014. FMDV replicons encoding green fluorescent protein are replication competent. J Virol Methods 209:35-40.

58. Newman J, Asfor AS, Berryman S, Jackson T, Curry S, Tuthill TJ. 2018. The Cellular Chaperone Heat Shock Protein 90 Is Required for Foot-and-Mouth Disease Virus Capsid Precursor Processing and Assembly of Capsid Pentamers. J Virol 92.